Electronic Supplementary Information

Tri-(Fe/F/N)-Doped Porous Carbons as Electrocatalysts for Oxygen Reduction Reaction in Both Alkaline and Acidic Media

Yongxing Diao[a,b], Hanmeng Liu[a,b], Zhixia Yao[a,b], Yaosheng Liu[a,b], Guangxing Hu[a,b], Qifang Zhang[a,d], Zhuang Li[a,b,c]*

[a] *State Key Laboratory of Electroanalytical Chemistry, Changchun Institute of Applied Chemistry, Chinese Academy of Sciences, Changchun, Jilin, 130022, China*
[b] *University of Science and Technology of China, Hefei, Anhui, 230026, China*
[c] *University of Chinese Academy of Sciences, Beijing, 100049, China*
[d] *College of Chemistry, Jilin Normal University, Siping, Jilin, 136000, China*
* *Corresponding Author.* Fax/Tel: +86-431-85262057;
E-mail: zli@ciac.ac.cn.

Experimental

1. Materials

Zinc nitrate hexahydrate ($Zn(NO_3)_2 \cdot 6H_2O$) was bought from Xilong Chemical Industry Co., Ltd. Iron(III) acetylacetonate ($Fe(acac)_3$) was purchased from Macklin Biochemical Co., Ltd. 2-Methylimidazole (2-mIM) was received from Aladdin Industrial Inc. Ammonium fluoride (NH_4F), potassium hydroxide (KOH), perchloric acid ($HClO_4$), methanol, and ethanol were purchased from Beijing Chemical Factory. Pt/C catalyst (20 wt% Pt on carbon-support) was bought from Alfa Aesar. Nafion solution (5 wt%) was obtained from Sigma-Aldrich. All chemicals were used without further purification. Ultrapure water used in all the experiments was produced by an ultrapure water machine.

2. Synthesis of ZIF-8 and Fe-ZIF-8

In a typical procedure, 60 mL of 0.1 M $Zn(NO_3)_3$ solution was prepared in methanol as solution A, and 120 mL of 0.2 M 2-methylimidazole solution (containing 1.32 g of $Fe(acac)_3$ when preparing Fe-ZIF-8) was prepared in methanol as solution B. Solution A was poured into solution B and stirred vigorously at 25 °C for 24 h. The resulting product was centrifuged, washed with methanol several times, and dried under vacuum at 60 °C overnight.

3. Synthesis of NC, FeNC, and FeFNC-X

Typically, ZIF-8 or Fe-ZIF-8 powder was transferred to a porcelain boat

and placed in a tube furnace. The samples were heated to 950 °C and maintained at 950 °C for 1 h, with a temperature increase rate of 5 °C min^{-1}, continuous flow under N_2 atmosphere, and then naturally cooled to room temperature. After that, a given amount of the obtained FeNC powder and NH_4F were dispersed ultrasonically in 10 mL H_2O. The mixture was stirred for 12 h and freeze-dried. Then the ground resulting powder was pyrolysed at 400 °C for 30 min, 900 °C for 1 h with a temperature increase rate of 5 °C min^{-1} under a continuous flow of N_2 atmosphere and then naturally cooled to room temperature, then pretreated in 1 M HNO_3 to remove unstable substances. In this work, the mass ratio of NH_4F and FeNC was set to be 1, 3, 5, 10, 20 to investigate the effect of different F content on ORR performance. As a result, the F doped samples were denoted as FeFNC-1, FeFNC-3, FeFNC-5, FeFNC-10, and FeFNC-20, respectively.

4. Material characterization

The morphology and composition characterizations were obtained by scanning electronic microscopy (SEM, XL-30 ESEM FEG), transmission electron microscopy (TEM, Thermo Fischer Talos F200x), X-ray diffraction (XRD, D8 ADVANCE), X-ray photoelectron spectroscopy (XPS, Thermo Electron Corp. ESCALABMK II equipped with Al Kαexciting source), Raman spectroscopy (Renishaw 2000, 514.5 nm excitation wavelength). Nitrogen adsorption and desorption isotherms were obtained at 77 K with a surface area analyzer (ASAP 2020,

Micromeritics, USA) based on the Brunauer-Emmet-Teller (BET) theory.

5. Electrochemical measurements

All electrochemical measurements were conducted with a three-electrode system on a CHI 832D electrochemical analyzer at room temperature. Platinum plate (1 cm^2), saturated calomel electrode (SCE), and rotating disk electrode (RDE, 4 mm in diameter) were selected as the counter electrode, reference electrode, and working electrode, respectively. In this study, all potentials were measured on the SCE reference electrode and converted to a reversible hydrogen electrode (RHE) reference scale by $E_{(RHE)} = E_{(SCE)} + 0.059$ pH $+ 0.241$. The catalyst ink was prepared by 5 mg catalyst dispersed 475 μL ethanol and 25 μL Nafion (5 wt%) solution and sonication for 30 min, then dropped the ink on a glassy carbon RRDE with a loading of 0.6 mg cm^{-2} to form catalyst film coated electrode and drying in air. For comparison, commercially available 20 wt% Pt/C catalysts were used. The Pt-based ink was obtained in the same way, yielding an approximate mass loading of 80 μg$_{Pt}$ cm^{-2}. The catalytic route of the catalyst can be evaluated according to the H_2O_2 yield and the electron transfer number (n). The H_2O_2 yield and electron transfer number (n) can be calculated by using the following equations:

$$H_2O_2(\%) = 200 \times \frac{j_R/N}{j_D + j_R/N}$$

$$n = 4 \times \frac{j_D}{j_D + j_R/N}$$

Where j_R is the ring current density and j_D is the disk current density. N equals to 0.42 as the current collection efficiency of the Pt ring. The kinetics parameters of ORR can be analyzed using the Koutecky-Levich (K-L) equation shown as follows:

$$\frac{1}{j} = \frac{1}{j_K} + \frac{1}{j_L} = \frac{1}{j_K} + \frac{1}{B\omega^{1/2}}$$

$$B = 0.62nFC_0(D_0)^{2/3}v^{1/6}$$

Where j is the measured current density, j_K and j_L are the kinetic and diffusion-limited current density, ω is the electrode rotation rate, F is the Faraday constant (96485 C mol^{-1}), C_0 is the bulk concentration of O_2 (1.3×10^{-3} mol L^{-1}), D_0 is the diffusion coefficient of O_2 (1.9×10^{-5} cm^2 s^{-1}) and v is the kinetic viscosity of the electrolyte (0.01 cm^2 s^{-1}).
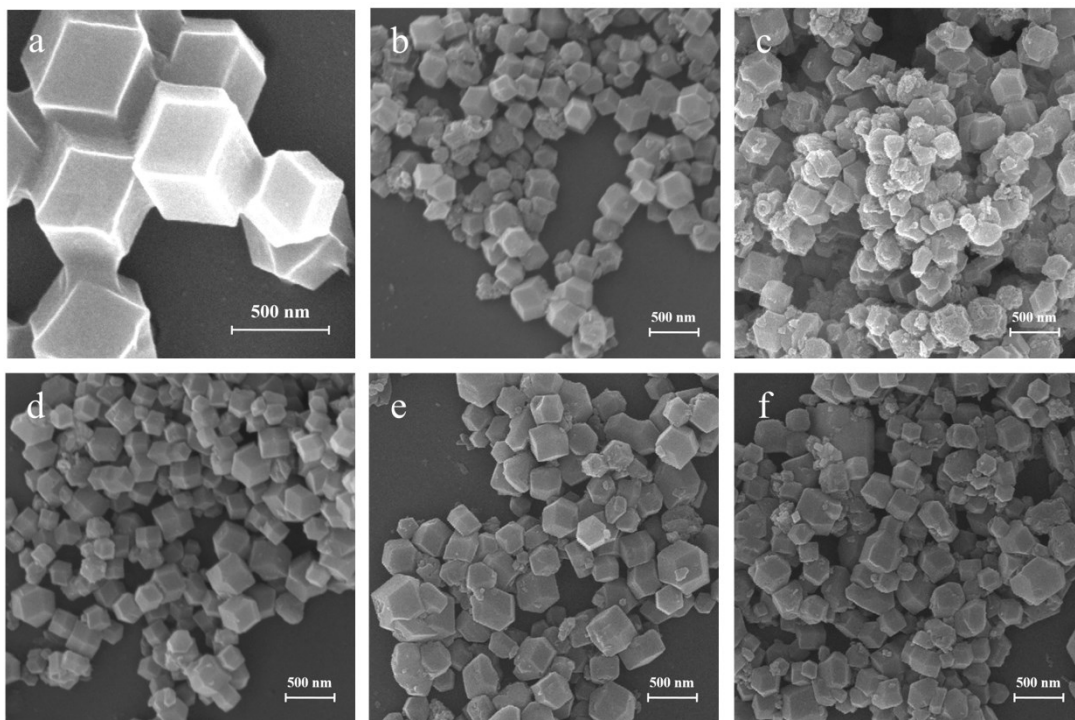
Fig. S1 SEM images of (a) Fe-ZIF-8, (b) FeNC, (c-f) FeFNC-X (X=1, 3, 10, 20).
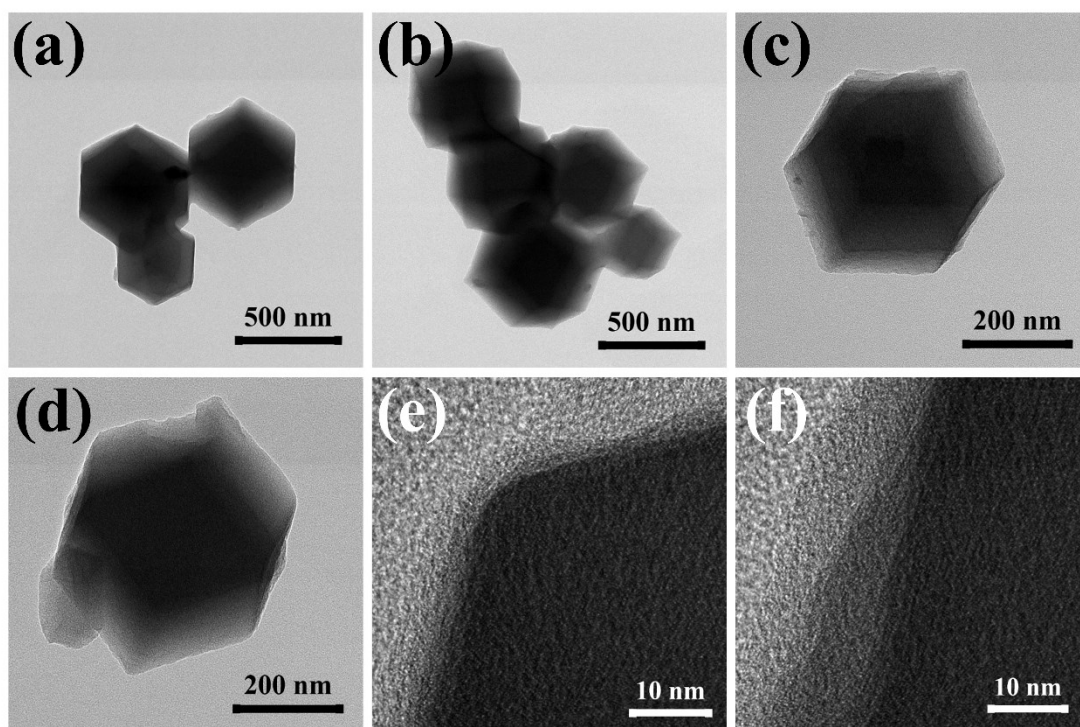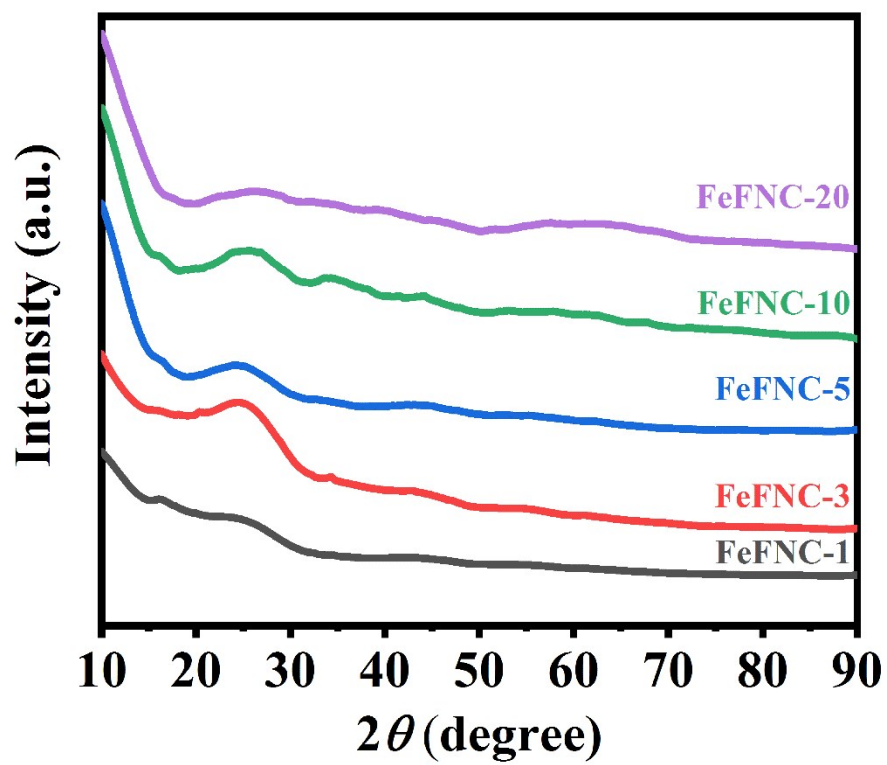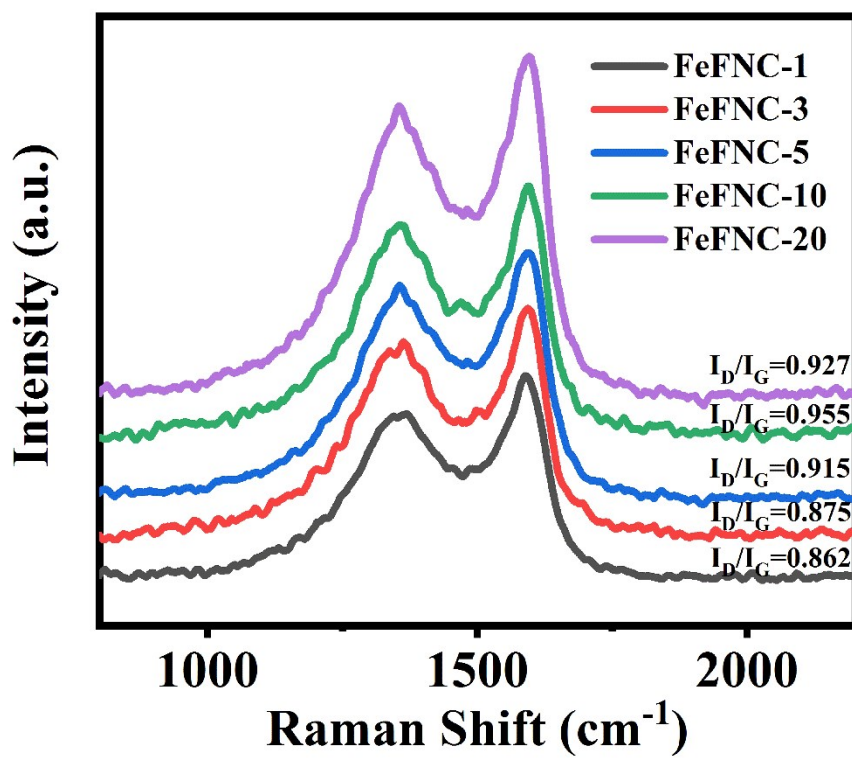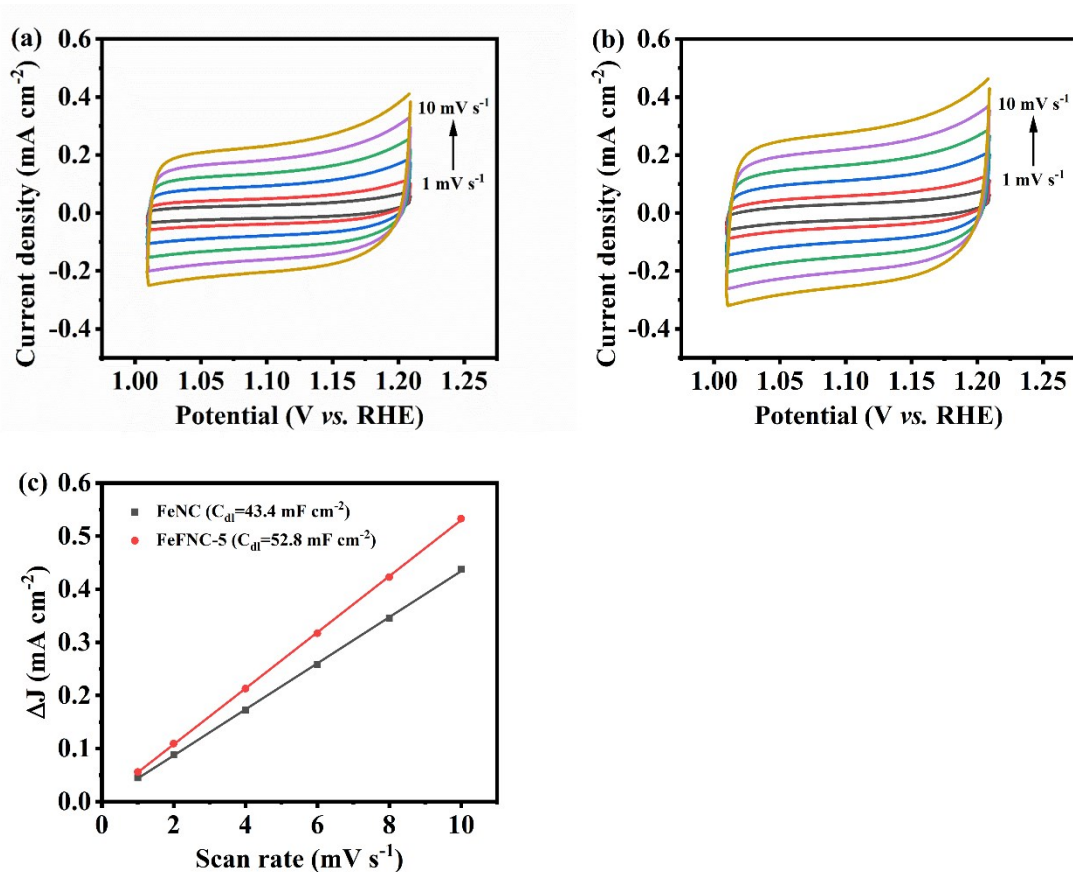
Fig. S2 (a-d) TEM and (e-f) HR-TEM images of FeFNC-5.

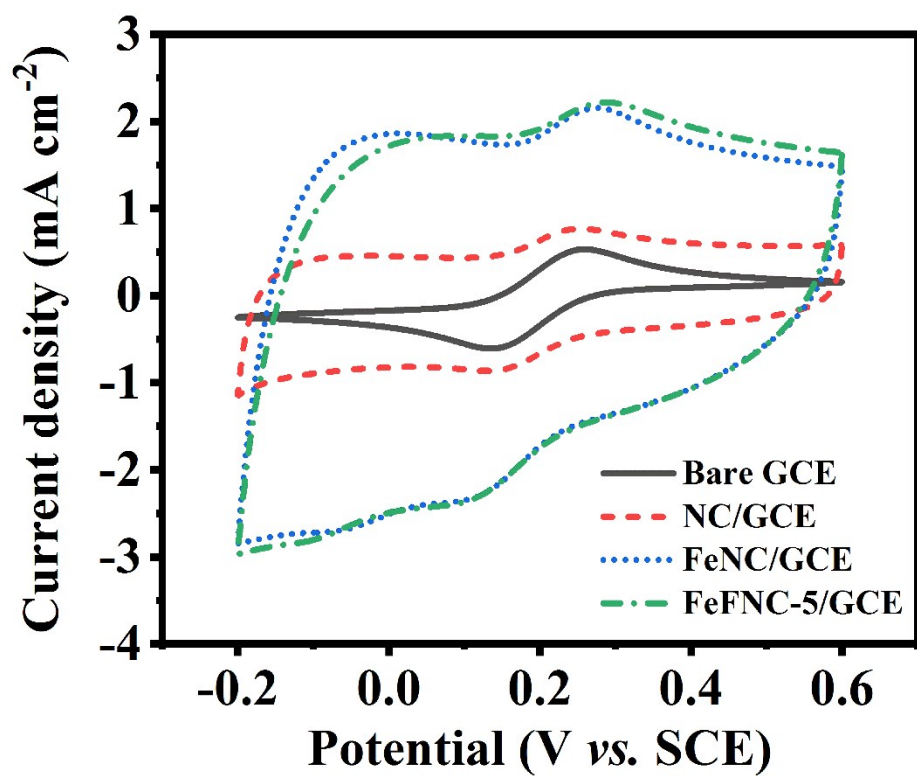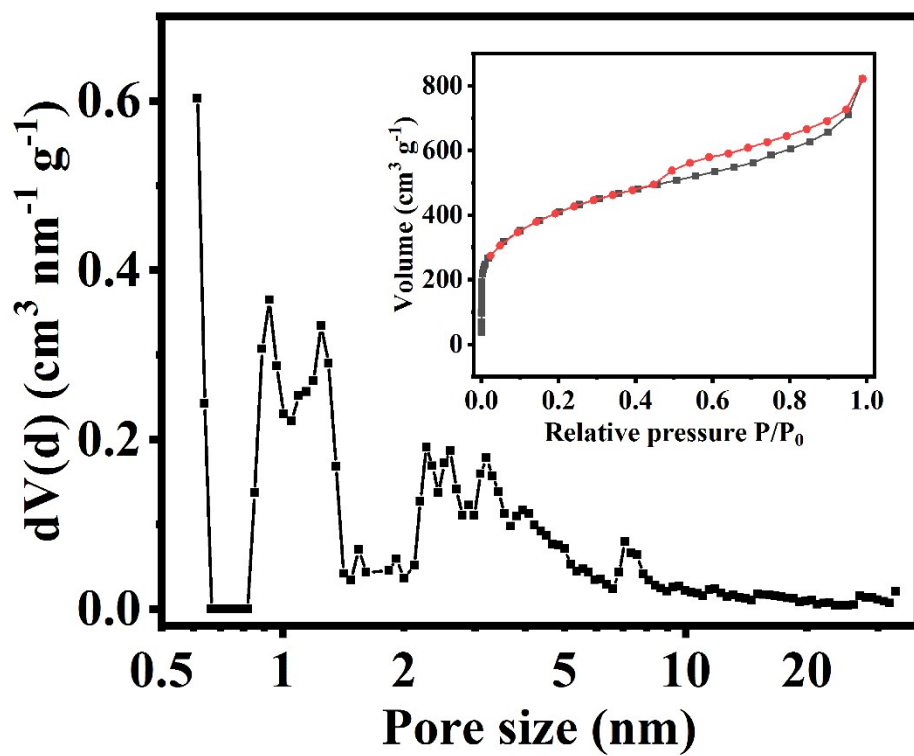**Fig. S3** XRD patterns of FeFNC-X (X=1, 3, 5, 10, 20).

Fig. S4 Raman spectra of FeFNC-X (X=1, 3, 5, 10, 20).
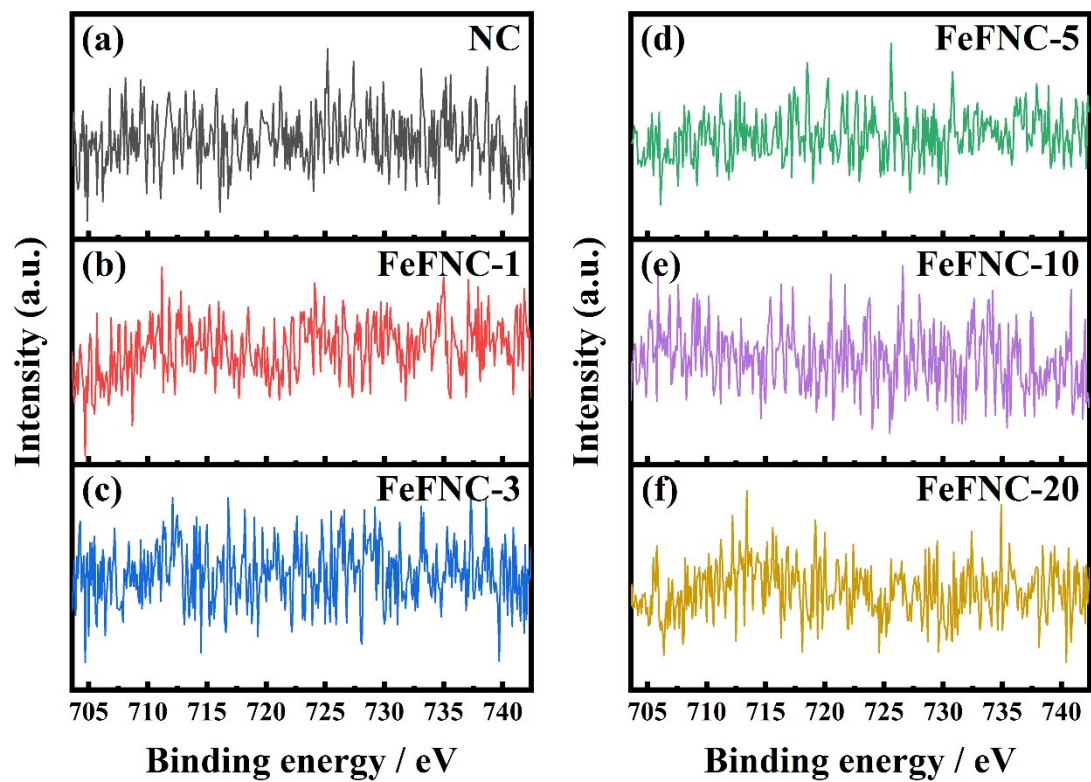
Fig. S5 CV curves of (a) FeNC and (b) FeFNC-5 at different scan rates of 1, 2, 4, 6, 8, and 10 mV s^{-1}, respectively. (c) Plots between current density difference (ΔJ) and scan rates at 0.2 V (vs. RHE).

Fig. S6 CV curves of bare GCE, NC, FeNC, and FeFNC-5 in 5.0 mM $[Fe(CN)_6]^{3-/4-}$ containing 0.10 M KCl.

Fig. S7 Pore size distribution and (inset) nitrogen adsorption-desorption isotherms of FeNC.

Fig. S8 The high resolution Fe 2p XPS spectra of (a) NC and (b-f) FeFNC-X (X=1, 3, 5, 10, 20).
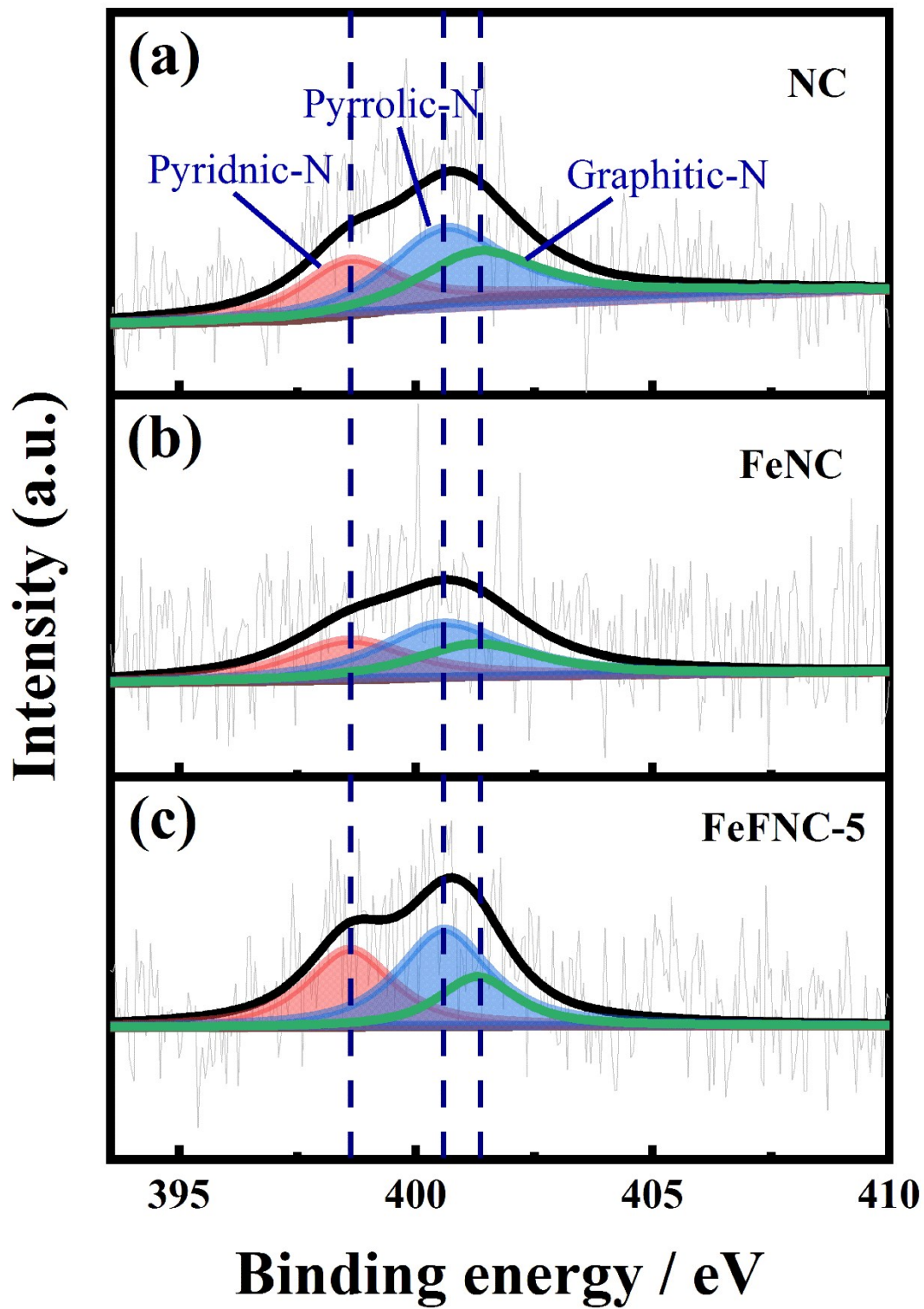
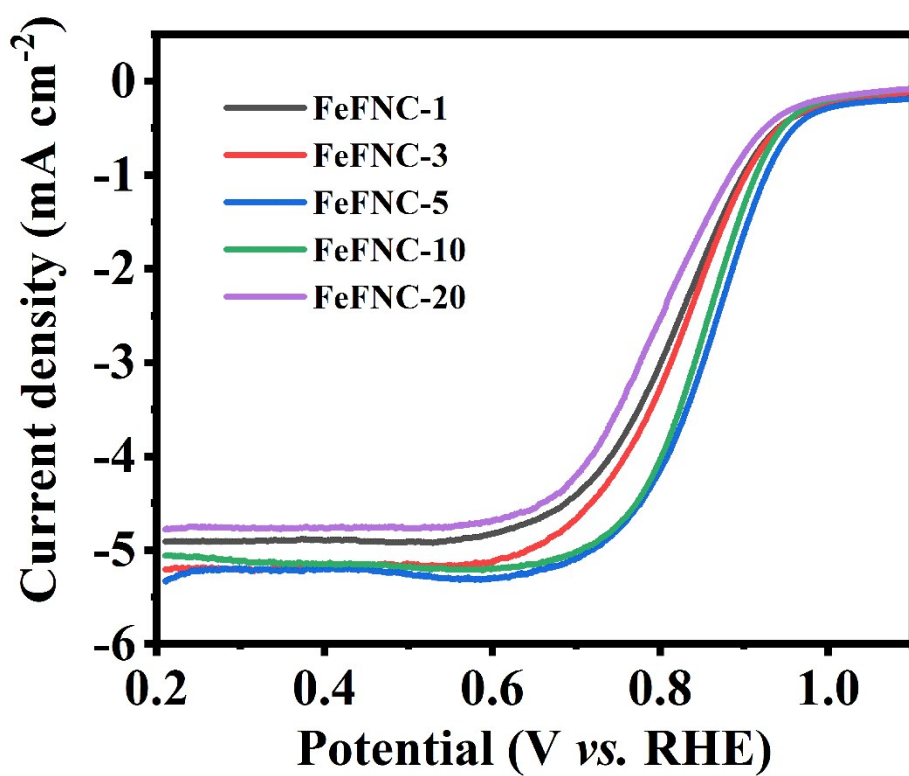**Fig. S9** The high resolution N 1s XPS spectra of (a) NC, (b) FeNC, and (c) FeFNC-5.

Fig. S10 LSV curves of FeFNC-X (X=1, 3, 5, 10, 20).
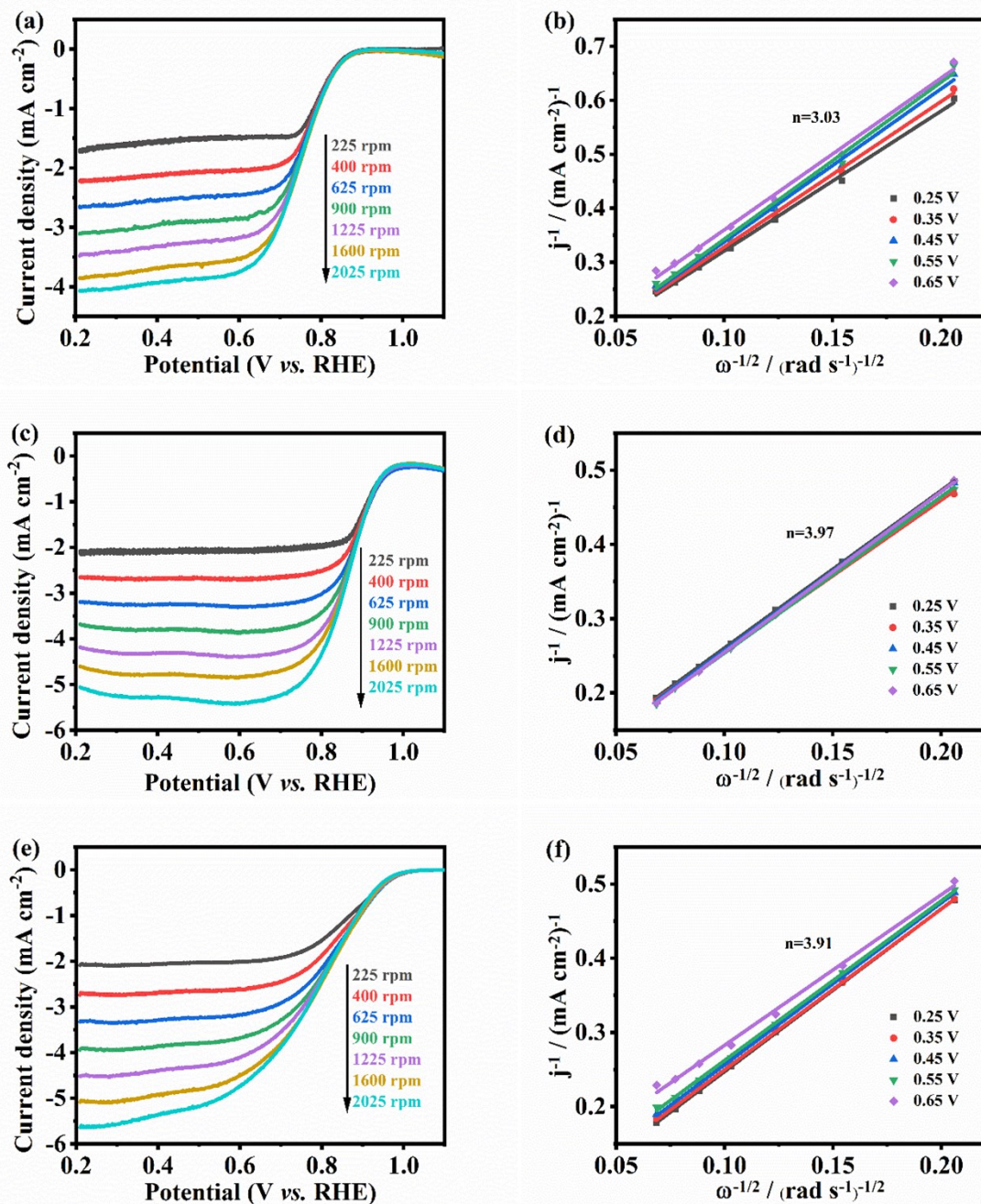
Fig. S11 RDE voltammograms of (a) NC, (c) FeFNC-5, and (e) Pt/C in O_2-saturated 0.1 M KOH under different rotational speeds with a sweep rate of 5 mV s^{-1}. The corresponding Koutecky-Levich plots of (b) NC, (d) FeFNC-5, and (f) Pt/C at the different potentials.
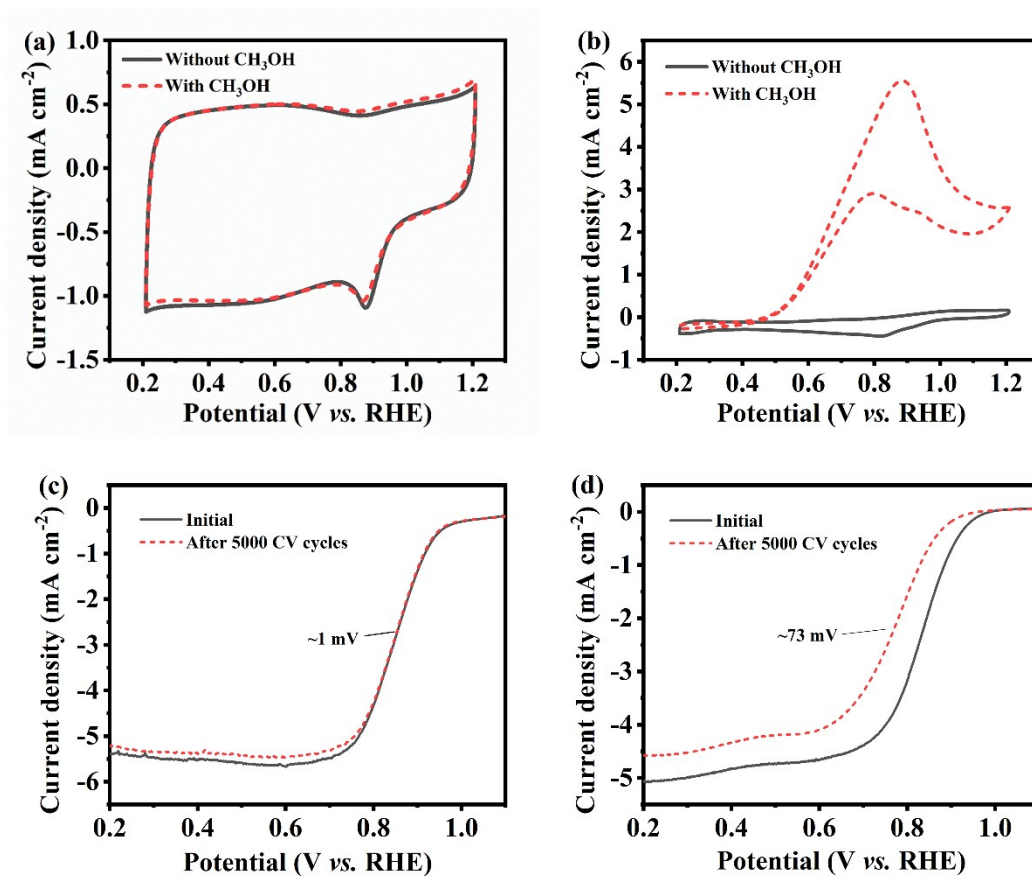
Fig. S12 The tolerance and stability of FeFNC-5 and Pt/C. The tolerance of (a) FeFNC-5 and (b) Pt/C to methanol in an O₂-saturated 0.1 M KOH solution at scan rate of 10 mV s⁻¹. The long-term operational stability of (c) FeFNC-5 and (d) Pt/C.
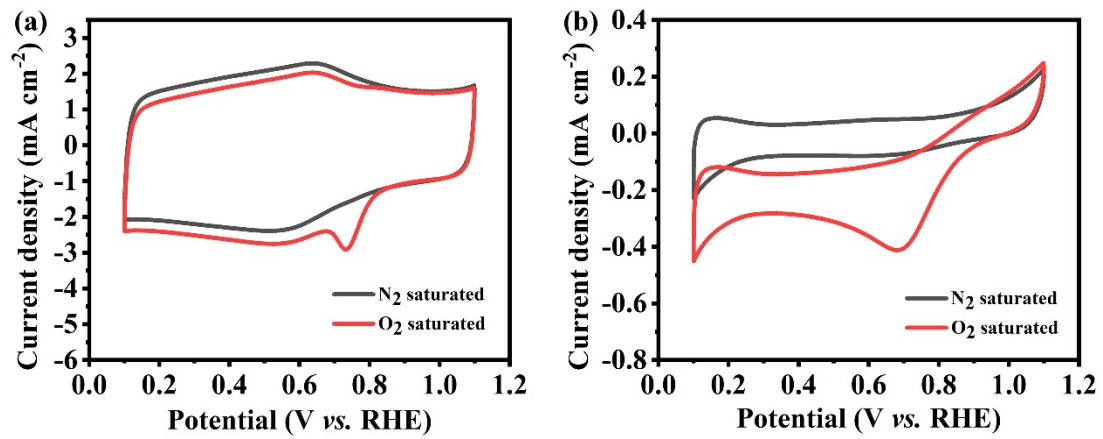
Fig. S13 CV curves of (a) FeFNC-5 and (b) Pt/C in N_2-saturated and O_2-saturated 0.1 M $HClO_4$ at scan rate of 20 mV s^{-1}.
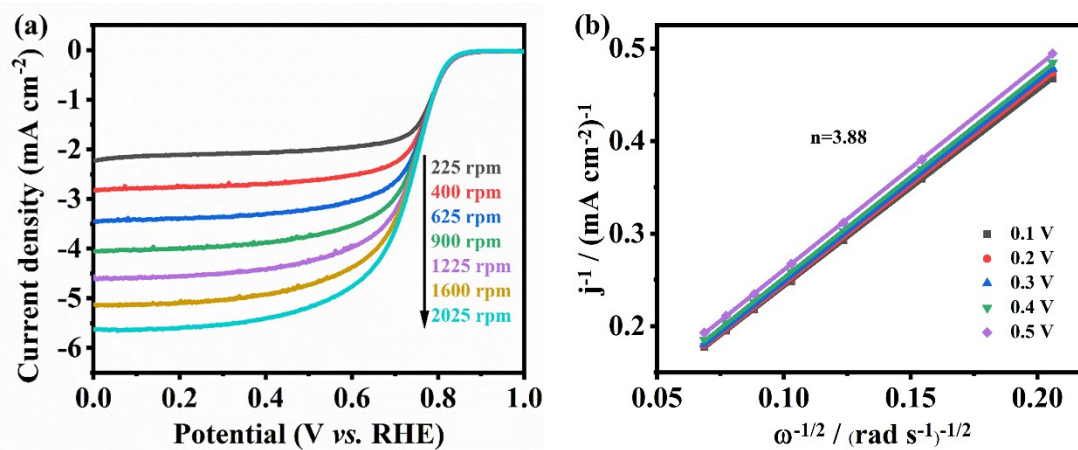
Fig. S14 (a) RDE voltammograms of FeFNC-5 under different rotational speeds with a sweep rate of 5 mV s^{-1} in O$_2$-saturated 0.1 M HClO$_4$ and (b) the corresponding Koutecky-Levich plots at the different potentials.
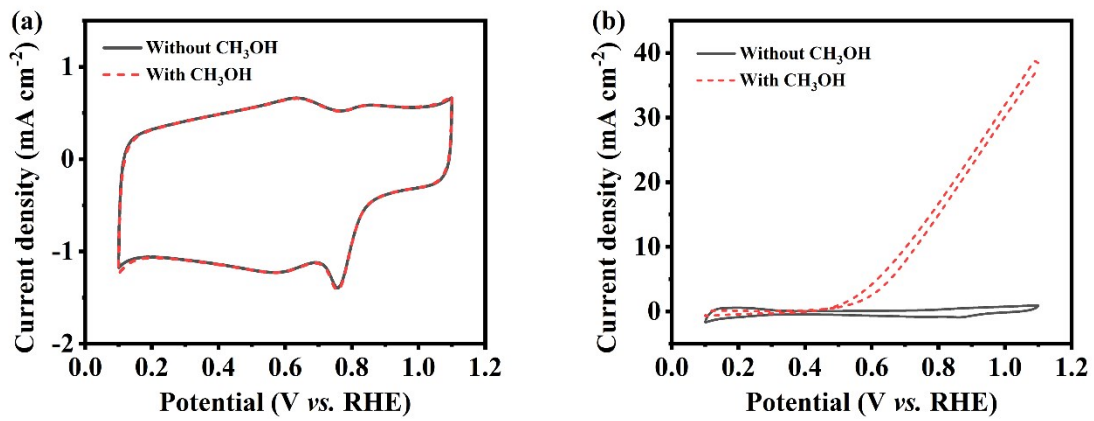
Fig. S15 The tolerance of (a) FeFNC-5 and (b) Pt/C to methanol in an O_2-saturated 0.1 M $HClO_4$ solution at scan rate of 10 mV s^{-1}.

Table S1 Summary of porosity parameters of NC, FeNC, and FeFNC-5.

Samples	BET SSA ($m^2\ g^{-1}$)	Pore volume ($cm^3\ g^{-1}$)	Pore diameter (nm)
NC	1037	1.214	4.685
FeNC	1390	1.271	3.658
FeFNC-5	792.9	0.8142	4.108

Table S2 Elemental composition of all samples obtain from XPS spectra.

Samples	C (at. %)	O (at. %)	N (at. %)	F (at. %)	Fe (at. %)
NC	86.16	10.29	3.55	-	-
FeNC	81.81	17.24	0.95	-	-
FeFNC-1	84.26	10.43	5.04	-	0.26
FeFNC-3	83.33	14.26	2.24	-	0.18
FeFNC-5	86.38	11.80	1.69	0.12	-
FeFNC-10	81.83	17.08	0.91	0.17	-
FeFNC-20	75.88	21.54	0.70	1.75	0.14

Table S3 Comparison of ORR performance in alkaline medium for FeFNC-5 with other non-noble metal heteroatom doped carbon electrocatalysts.

Catalyst	E_{onset}/V	$E_{1/2}$/V	Reference electrode	References
Fe/N/F-MCNF	0.900	0.822	vs. RHE	[1]
Co-Fe/NC-700	-	0.854	vs. RHE	[2]
Fe@NMC-1	1.01	0.876	vs. RHE	[3]
NHPC$_{1:3}$-900	-	0.87	vs. RHE	[4]
FeCo@C MS	1.04	0.85	vs. RHE	[5]
Co-N-C/CoO$_x$-3	-	0.82	vs. RHE	[6]
FeCo-NC-850	0.997	0.864	vs. RHE	[7]
Co/NCNT/NG	0.96	0.85	vs. RHE	[8]
A-Co/r-GOs (Zn$_{10}$Co$_1$)	0.974	0.825	vs. RHE	[9]
Fe-N-C-1	-0.061	-0.171	vs. Ag/AgCl	[10]
20 wt% Pt/C	0.980	0.852	vs. RHE	this work
FeFNC-5	0.976	0.872	vs. RHE	this work

Table S4 Comparison of ORR performance in acidic medium for FeFNC-5 with other non-noble metal heteroatom doped carbon electrocatalysts.

Catalyst	E_{onset} vs. RHE	$E_{1/2}$ vs. RHE	Electrolyte	References
LN-3-1	0.892	0.792	1 M $HClO_4$	[11]
PyN-GDY	0.81	0.55	0.1 M $HClO_4$	[12]
Co–N–C@F127	0.93	0.84	0.5 M H_2SO_4	[13]
NFLGDY-900c	-	0.73	0.1 M $HClO_4$	[14]
SA-Fe-HPC	-	0.81	0.1 M H_2SO_4	[15]
SA-Fe/NG	0.9	0.8	0.5 M H_2SO_4	[16]
Fe-N-C-950	0.92	0.78	0.1 M $HClO_4$	[17]
Cu@Fe-N-C	0.88	0.761	0.5 M H_2SO_4	[18]
20Co-NC-1100	0.93	0.8	0.5 M H_2SO_4	[19]
Mn-NC-second	-	0.8	0.5 M H_2SO_4	[20]
20 wt% Pt/C	0.865	0.748	0.1 M $HClO_4$	this work
FeFNC-5	0.826	0.749	0.1 M $HClO_4$	this work

Notes and references

1. Y. G. Lee and H. J. Ahn, *Appl. Surf. Sci.*, 2019, **487**, 389-397.
2. S. L. Zhang, B. Y. Guan and X. W. D. Lou, *Small*, 2019, **15**, 1805324.
3. X. D. Chen, N. Wang, K. Shen, Y. K. Xie, Y. P. Tan and Y. W. Li, *ACS Appl. Mater. Inter.*, 2019, **11**, 25976-25985.
4. C. J. Xuan, B. S. Hou, W. W. Xia, Z. K. Peng, T. Shen, H. L. Xin, G. A. Zhang and D. L. Wang, *J. Mater. Chem. A*, 2018, **6**, 10731-10739.
5. Y. T. Xu, B. L. Chen, J. Nie and G. P. Ma, *Nanoscale*, 2018, **10**, 17021-17029.
6. W. L. Xin, K. K. Lu and D. Shan, *Appl. Surf. Sci.*, 2019, **481**, 313-318.
7. G. N. Li, K. T. Zheng and C. J. Xu, *Appl. Surf. Sci.*, 2019, **487**, 496-502.
8. L. Yang, Y. L. Lv and D. P. Cao, *J. Mater. Chem. A*, 2018, **6**, 3926-3932.
9. L. J. Zhang, T. C. Liu, N. Chen, Y. Jia, R. S. Cai, W. Theis, X. F. Yang, Y. Z. Xia, D. J. Yang and X. D. Yao, *J. Mater. Chem. A*, 2018, **6**, 18417-18425.
10. X. Xin, H. L. Qin, H. P. Cong and S. H. Yu, *Langmuir*, 2018, **34**, 4952-4961.
11. Y. Shen, Y. Li, G. Yang, Q. Zhang, H. Liang and F. Peng, *J. Energy Chem.*, 2020, **44**, 106-114.
12. Q. Lv, N. Wang, W. Si, Z. Hou, X. Li, X. Wang, F. Zhao, Z. Yang, Y. Zhang and C. Huang, *Appl. Catal. B-Environ.*, 2020, **261**, 118234.
13. Y. He, S. Hwang, D. A. Cullen, M. A. Uddin, L. Langhorst, B. Li, S. Karakalos, A. J. Kropf, E. C. Wegener, J. Sokolowski, M. Chen, D. Myers, D. Su, K. L. More, G. Wang, S. Litster and G. Wu, *Energ. Environ. Sci.*, 2019, **12**, 250-260.
14. Y. Zhao, J. Wan, H. Yao, L. Zhang, K. Lin, L. Wang, N. Yang, D. Liu, L. Song, J. Zhu, L. Gu, L. Liu, H. Zhao, Y. Li and D. Wang, *Nat Chem*, 2018, **10**, 924-931.
15. Z. Zhang, J. Sun, F. Wang and L. Dai, *Angew. Chem. Int. Ed. Engl.*, 2018, **57**, 9038-9043.
16. L. Yang, D. Cheng, H. Xu, X. Zeng, X. Wan, J. Shui, Z. Xiang and D. Cao, *Proc Natl Acad Sci U S A*, 2018, **115**, 6626-6631.
17. M. Xiao, J. Zhu, L. Ma, Z. Jin, J. Ge, X. Deng, Y. Hou, Q. He, J. Li, Q. Jia, S. Mukerjee, R. Yang, Z. Jiang, D. Su, C. Liu and W. Xing, *ACS Catal.*, 2018, **8**, 2824-2832.
18. Z. Wang, H. Jin, T. Meng, K. Liao, W. Meng, J. Yang, D. He, Y. Xiong and S. Mu, *Adv. Funct. Mater.*, 2018, **28**, 1802596.
19. X. X. Wang, D. A. Cullen, Y. T. Pan, S. Hwang, M. Wang, Z. Feng, J. Wang, M. H. Engelhard, H. Zhang, Y. He, Y. Shao, D. Su, K. L. More, J. S. Spendelow and G. Wu, *Adv. Mater.*, 2018, **30**, 1706758.
20. J. Li, M. Chen, D. A. Cullen, S. Hwang, M. Wang, B. Li, K. Liu, S. Karakalos, M. Lucero, H. Zhang, C. Lei, H. Xu, G. E. Sterbinsky, Z. Feng, D. Su, K. L. More, G. Wang, Z. Wang and G. Wu, *Nat. Catal.*, 2018, **1**, 935-945.